Direct access to the order parameter: Parameterized symmetry modes and rigid body movements as a function of temperature

M. Müller, R.E. Dinnebier, N.Z. Ali and M. Jansen

Introduction

Many crystalline phases can be viewed as low-symmetry distortions of real or hypothetical higher-symmetry parent structures (i.e., aristotypes). In such cases, a group-subgroup relationship must exist between the two structures, so that all symmetry elements of the low-symmetry phase are also present in the high-symmetry phase. The low-symmetry phase will generally have more structural degrees of freedom than the parent phase, and may involve some combination of magnetic, displacive, occupancy and strain degrees of freedom. Using group-representation theory, these degrees of freedom can always be parameterized in terms of basis functions of the irreducible representations (irreps) of the parent symmetry, which we refer to as symmetry-adapted distortion modes, or more simply as symmetry-modes. The symmetry modes of a given type (e.g., lattice strain, displacive, occupancy or magnetic) belonging to the same irrep collectively comprise an 'order parameter'. The key order parameters that define a structural transition have zero amplitude on the high-symmetry side, and take on non-zero amplitudes on the low-symmetry side. These order parameters tend to place the daughter atoms of a given parent atom onto more general Wyckoff sites and often split a parent atom across multiple unique daughter sites. In many cases, the symmetry-adapted description is the most natural parameter set, because nature's order parameters are usually selected to break a specific set of symmetries.

In case of framework crystal structures, whose structural distortions involve rigid polyhedral units, the most natural description comprises tilt modes that leave the polyhedra undistorted. To account for this additional chemical information, one uses rotations, translations, and torsions as adjustable parameters. If the voids of the framework are occupied by guest atoms or molecules, these entities may also translate and/or reorient. The rigid-body (RB) description is more restrictive than the symmetry-mode (SM) basis, which is helpful when only RB behavior is observed. But a single symmetry-adapted order parameter will often approximate a rigid-body mode for small mode amplitudes; and a linear combination of symmetry modes can achieve any possible distortion, including RB distortions.

If the distorted structure has a lower point group symmetry than the parent structure, the distortion can be referred to as ferroic. A ferroic distortion can be further classified as ferroelastic if it changes the shape of the unit cell in such a way as to alter the crystal system. A ferroelastic distortion can be described in terms of spontaneous macroscopic strains (ε_s) of the parent unit cell parameters. The ferroelastic transition then marks the boundary between the low-symmetry ferroelastic phase and a higher-symmetry paraelastic phase that supports only disordered local strains. Landau theory describes the main physical features of most ferroelastic phase transitions, wherein the thermodynamic state of the system and the free-energy difference that stabilizes the low-symmetry phase (the excess Gibbs free energy) are expressed in terms of thermodynamic order parameters [1]. Here, we will treat the lattice strains as linear combinations of symmetry-adapted gamma-point order parameters, which may also be coupled to additional displacive order parameters.

In Landau theory, an order parameter decreases continuously to zero at a second-order (a.k.a. continuous) phase transition, whereas an order parameter can abruptly 'jump' to a non-zero value at a first-order (a.k.a. hysteretic) transition. For a continuous transition, the order parameter's dependence on temperature can be modeled by an empirical power law of the form

$$Q = f \mid T_{crit} - T \mid^{\beta} \quad (2)$$

where T_{crit} is the transition temperature, β is the critical exponent, and f is a temperature coefficient. Typical values of β are 1/2 for ordinary scalar second-order transitions, or 1/4 for a transition at the tricritical point that marks the boundary between first and second-order transitions. Values between 1/4 and 1/2 might be obtained for a variety of reasons. The Landau critical exponent is derived by calculating the first derivative of the power series expansion of a truncated Gibbs free energy with respect to the order parameter and setting it to zero, a simplistic approach that is really only valid in a small temperature interval around T_{crit}. But near a tricritical point, one obtains $\beta \approx 1/4$ for temperatures near T_{crit}, $\beta \approx 1/2$ for temperatures far below T_{crit}, and an intermediate 'effective' value when attempting to fit over an extended temperature range that includes both extremes. However, it has also been shown that non-standard power-law exponents obtained from fits over extended temperature ranges are often due to temperature-dependent energy-expansion coefficients of order four or higher and have nothing at all to do with critical phenomena. And finally, attempting to fit a power-law to an order parameter that is only approximately second order, will artificially suppress the exponent do to the unusually rapid descent near the transition.

The most common method of characterizing structural phase transitions is the powder X-ray or neutron diffraction. Modern lab instruments and advanced scattering facilities now provide for the rapid collection of high-resolution powder diffraction patterns as a function of parameters like temperature, pressure or simple time. 1D or 2D position sensitive detectors allow for efficient measurements of a series of powder pattern near a phase transition. Usually, powder diffraction patterns are refined individually, followed by a post-refinement analysis of lattice parameters or atomic coordinates as a function of external variables. But with the availability of flexible self-programmable Rietveld programs like TOPAS, the simultaneous refinement of a single parametric model against multiple data sets has now become possible [2]. User-friendly software packages that allow one to automatically re-parameterize a low-symmetry structure in terms of symmetry-adapted order parameters of a higher symmetry structure have also become available (e.g., ISODISPLACE [3,4] and AMPLIMODES), and require only a very basic knowledge of group theory. Together, these developments have enabled fast and stable parametric refinements of physically-meaningful order parameters that were previously impractical.

Here, the ferroelastic phase transition of $CsFeO_2$ is investigated in detail via parametric Rietveld refinement as a function of temperature. Both displacive and strain order parameters are modeled using power-law trends below T_{crit}. The displacive order parameters are analyzed using both the RB and SM descriptions for comparison purposes.

Method

Both RB and SM distortion models have been used to study the ferroelastic phase transition of $CsFeO_2$ from a cubic (space group $Fd\bar{3}m$) parent structure to an orthorhombic (space group *Pbca*) low-symmetry structure (Fig. 13). We describe the SM approach first. Starting with $Fd\bar{3}m$ and *Pbca* CIF-structure files that were derived from single-crystal X-ray diffraction data from isotypic $RbFeO_2$ [5], the ISODISPLACE software was used to perform an automatic symmetry-mode decomposition of the low-symmetry distorted structure into modes of the high-symmetry cubic parent. In the cubic phase, despite having a total of 32 atoms in the conventional face-centered unit cell, the structure of $CsFeO_2$ has no free atomic coordinates.

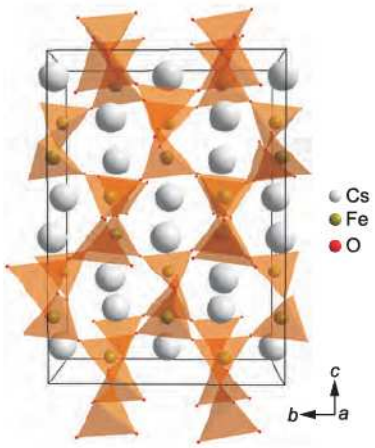

Figure 13: An *a*-axis projection of the low-temperature (*Pbca*) crystal structure of $CsFeO_2$.

The cubic cell contains one unique atom of each type, each of which lies on a special Wyckoff point. In the orthorhombic phase, however, there are 24 free atomic coordinates. Because the symmetry-mode basis is related to the traditional atomic-coordinate basis by a linear transformation, there must also be 24 displacive symmetry modes. For convenience, we number these modes from 1 to 24.

Equation (3) shows how the atomic positions $\mathbf{r}_j$ of the low-symmetry (LS) and high-symmetry (HS) phases are related.

$$\mathbf{r}_j^{LS} = \mathbf{r}_j^{HS} + \sum_m c_{j,m}\, Q_m\, \varepsilon(j\,|\,m) \qquad (3)$$

The j index indicates an atom in the low-symmetry supercell, the m index runs over all of the modes associated with its parent atom, $\varepsilon(j\,|\,m)$ is the j^{th} component of the unnormalized (i.e., nice-looking) polarization vector of the m^{th} mode, and the $c_{j,m}$ are normalization coefficients such that $\sum_j c_{j,m}^2\, \varepsilon(j\,|\,m)^2 = 1$. Q_m is the amplitude of the m^{th} mode, and equals the root-summed-squared displacement, summed over all supercell atoms affected by the mode. ISODISPLACE essentially used group-theoretical methods to compute the symmetry-mode polarization vectors and normalization coefficients, and then saved the results as a system of linear equations in TOPAS.str format [3].

Ten of the 24 displacive symmetry modes were identified as being necessary to describe the phase transition: two ($a2$ and $a4$) for caesium, two ($a9$ and $a10$) for iron and six ($a14$, $a15$, $a16$, $a17$, $a18$ and $a19$) for oxygen. The $a2$-mode affects the y-coordinates of both Cs atoms, while $a4$ only affects the x-coordinate of Cs_2. The $a10$ mode influences the y-coordinate of the Fe1 and Fe2 atoms while the $a10$ mode influences only the x-coordinate of the Fe1 atom. Oxygen modes $a14$ to $a19$ cooperate to describe the rotation of the FeO_4 tetrahedron, which should not be substantially distorted.

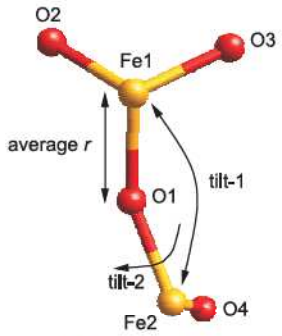

Figure 14: Rigid body consisting of the crystallographically independent atoms of the structure building double tetrahedron in $CsFeO_2$ exhibiting three internal parameters: *r*, tilt-1 and tilt-2.

Next, we describe implementation of the rigid-body model, in which the low-symmetry distortion was defined in terms of polyhedral tilt angles that left the polyhedra themselves undistorted. A suitable rigid building unit that describes both the low- and high-temperature $CsFeO_2$ structures consists of two regular corner-sharing FeO_4 tetrahedra that are tilted with respect to each other as shown in Fig. 14. Taking symmetry equivalent positions into account, the resulting rigid body consists of four oxygen and two iron atoms with two tilting angles and the average Fe–O distance (r) as internal degrees of freedom, as illustrated in Fig. 14. The two tilt angles are (1) the Fe1–O1–Fe2 (tilt-1) bond angle and (2) the O4–Fe2–O1-Fe1 tortion angle (tilt-2) between the two tetrahedra. For the Rietveld refinement, the rigid body was

set up in form of a z-matrix that naturally describes the position of each atom in terms of its distance, angle and torsion angle relative to previously defined atoms. The bridging O1 oxygen atom of the two tetrahedra was used as the center of the rigid body. The orientation and position of the rigid body relative to the internal coordinate system of the crystal was held constant over the entire temperature range of investigation and only the three internal degrees of freedom were subjected to refinement. As the two Cs atoms in the voids of the framework are independent of the rigid body, their crystallographically relevant atomic coordinates were refined separately.

The technique of parametric Rietveld refinement [2] was applied to both the SM and RB models. This technique enables the refinement of various (e.g., thermodynamic) parameters directly from diffraction data. Prior to parametric refinement, preliminary refinements were performed at each temperature individually, and the temperature dependence of each candidate symmetry mode or z-matrix parameter was examined in order to identify the parameter subset that captures the principle features of the distortion. Then, for the parametric refinement, these crystallographic structural parameters were not refined directly, but were rather modeled as power-law temperature trends (Eq. (2)), so that each one possessed a temperature-independent power-law exponent and coefficient [1]. Each z-matrix parameter in the RB model possessed an unique refinable coefficient and exponent. In the SM model, however, all modes belonging to a single order parameter (labeled according to irrep) shared the same power-law exponent. The temperature-independent power law exponents and coefficients were then subjected to parametric refinement, simultaneously against diffraction patterns collected at all temperatures. Topas (Version 4.1; Bruker AXS) was used to perform the refinements [6].

The characterization of the lattice strain below the ferroelastic phase transition is also important here. Strain is a symmetric second rank tensor that can be represented by a 3×3 matrix which for the orthorhombic symmetry (actual supercell) reduces to a diagonal matrix with the following diagonal elements:

$$
\begin{aligned}
e_{11s} &= \frac{a_s}{a_{s0}} - 1 = \frac{a_s}{a_{p0}/\sqrt{2}} - 1 \\
e_{22s} &= \frac{b_s}{b_{s0}} - 1 = \frac{b_s}{\sqrt{2}\, a_{p0}} - 1 \\
e_{33s} &= \frac{c_s}{c_{s0}} - 1 = \frac{c_s}{2\, a_{p0}} - 1
\end{aligned}
\tag{4}
$$

with the lattice parameters of the supercell a_s, b_s., c_s and the isothermal lattice constants a_{s0}, b_{s0} and c_{s0}. The isothermal lattice constants can be given as well in dependence on the isothermal lattice constant of the cubic parent cell a_{p0}.

In the present parametric refinements, the supercell strain parameters were modeled as power-law trends vs. temperature. They are viewed as independent coupled order parameters and each possesses their own power-law exponents and coefficients (Eq. 5). In the parametric refinement, a conditional statement defined the region below the transition where the order parameters were permitted to have non-zero values.

$$
\begin{aligned}
&\text{If } (T < T_{crit}) \quad \text{then } \varepsilon_\Gamma(T) = f_\Gamma (T_{crit} - T)^{\beta_\Gamma}, \\
&\qquad\qquad\quad \text{else} \qquad \varepsilon_\Gamma = 0
\end{aligned}
\tag{5}
$$

During parametric refinement the exponents and coefficients of the strain (Eq. (4)) were used to calculate the supercell lattice parameters at each temperature. It was necessary to treat the cubic parent cell parameter as a temperature-dependent quantity, $a_0(T)$, and to linearly extrapolate it into the region of the low-symmetry phase in order to correct for the additional effects of thermal expansion. The slope (m_0) and intercept (t_0) used for this extrapolation were also part of the parametric refinement.

Experiment

Powder diffraction measurements were performed at the Materials Sciences (MS-Powder) beamline of the Swiss Light Source using synchrotron radiation of a wavelength of 0.49701 Å using the Microstrip Detector Mythen-II.

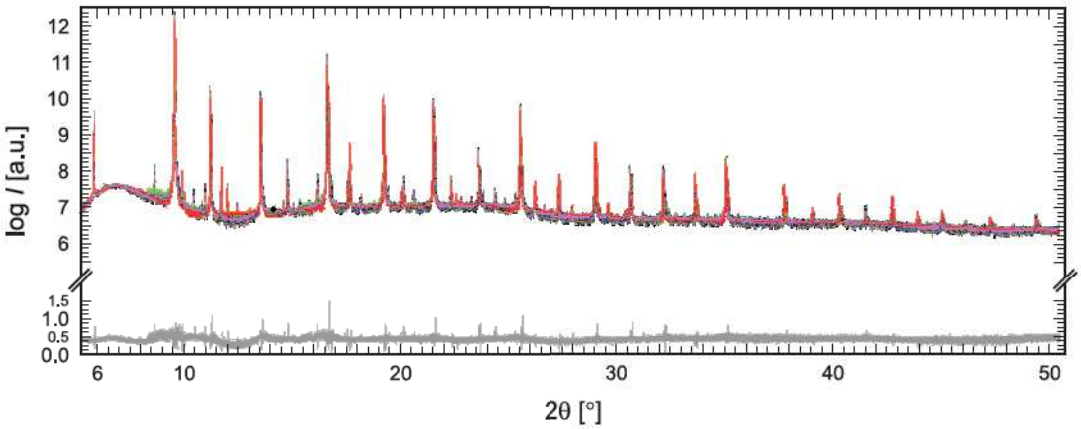

Figure 15: Logarithmic plot of temperature-dependent parametric symmetry-mode refinement of $CsFeO_2$ in the temperature ranges from 303 K to 409 K. Observed, calculated and difference traces for all temperatures used (1 K steps) are shown in a stacked arrangement.

The sample was sealed in a Hilgenberg quartz-glass capillary with a diameter of 0.3 mm. The diffraction patterns were collected on heating the powder sample from 303 K – 409 K with steps of 1 K using a STOE capillary furnace. The powder patterns were recorded for 40 seconds (4 scans of 10 seconds each) in the angular range from 3.0° – 53.38° 2θ.

Results and Discussion

The dependence of the crystal structure of $CsFeO_2$ on temperature in the temperature range from 303 K to 409 K was investigated by sequential and parametric Rietveld refinement. Both symmetry mode (SM) and rigid-body (RB) refinements were performed. Figure 15 illustrates the results from a temperature-dependent parametric symmetry-mode refinement against all available data sets throughout the temperature range investigated.

The parametric model produced diffraction patterns that agreed well with corresponding experimental patterns at each temperature, demonstrated the effectiveness of the parametric approach and the inclusion of an adequate structural-parameter set. Including additional parameters did not significantly improve the quality of the fit.

For both types of parametric Rietveld refinements (SM, RB) the lattice parameters varied only slightly. Below the phase transition, all strain order parameters (Fig. 16) and lattice parameters exhibit the anticipated power law trends, while above the transition, the lattice parameters can be adequately fitted using a linear function within the investigated temperature range. The strain order parameters exhibited essentially the same development when applied to the SM and RB models. Observe that the magnitude of the strain component e_{11} is significantly higher as the magnitudes of e_{22} and e_{33}, which are of comparable size.

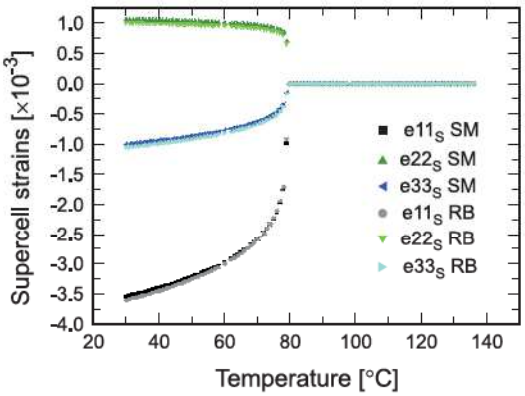

Figure 16: Temperature-dependent supercell strains for $CsFeO_2$ as calculated from their parametrically-refined power-law models.

The temperature dependencies of the displacive degrees of freedom are plotted in Fig. 17. These power-law curves were calculated using the parametrically-refined coefficients and exponents.

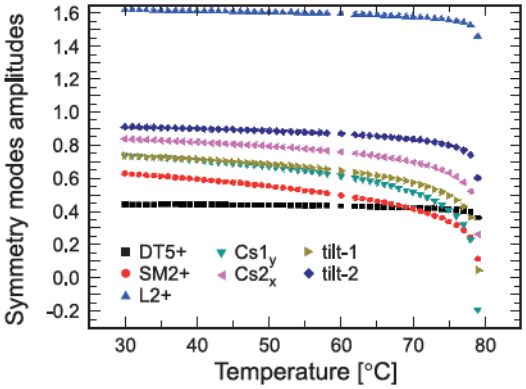

Figure 17: Comparison of the root squared sum of the DT5+, SM2+ and L2+ with the normalized internal RB parameters in dependence on temperature. Temperature-dependent symmetry-mode amplitudes for $CsFeO_2$ as calculated from their parametrically-refined power-law models.

If one views the set of all possible distortions possessing the requisite supercell and *Pbca* symmetry as a multi-parameter vector space, the traditional atomic-coordinate (TAC) and SM descriptions both span the entire distortion space.

In contrast, the RB description is much more restrictive because it only allows distortions that preserve the shapes of the rigid polyhedra. Thus the RB description has far fewer free parameters. While the SM description has just as much freedom as the TAC description, only a relatively small fraction of the available symmetry modes tend to be important to a specific phase transition. And in the case of $CsFeO_2$, a relatively small number of symmetry modes can approximately reproduce the rigid-body motions observed.

Ideally, we would expect all of the modes associated with a single symmetry-adapted order parameter to evolve together, sharing the same power-law exponent, and have assumed this to be the case in defining the SM model of $CsFeO_2$. The key displacive order parameters that contribute to the low-temperature $CsFeO_2$ distortion appear to be DT5+(Δ_5), SM2(Σ_2) and L2+(L_2^+). ISODISPLACE was used to determine that any two of these could comprise a potentially primary (i.e., capable of producing the symmetry of the distorted phase) pair of coupled order parameters. In general, coupled order parameters can arise at different temperatures and follow different trends. Or they can be strongly coupled, arising at nearly the same temperature and following very similar trends. Because sequential single-temperature refinements indicate that each of the important order parameters of $CsFeO_2$ arise within a 1 K temperature range, we assumed they all appear at the same temperature (352 K). Because the DT5, SM2 and L2+ order parameters must cooperate in order to preserve the shapes of the FeO_4 tetrahedra, we can reasonably assume that they are strongly coupled by physical bonding constraints. Thus, we might expect them to exhibit similar temperature evolutions. The $a15$ and $a19$ symmetry modes, for example, must cooperate to mimic the RB tilt-2 angle, and therefore are coupled with the same power-law exponents. Because the SM and RB models are roughly equivalent, it is not surprising that the DT5/L2+ power-law exponent is similar to that of the RB tilt-2 angle itself. Other relationships between the two models include the $a10$ symmetry mode, which approximates the RB tilt-1 angle, and the $a2$ and $a4$ symmetry modes which are related to the Cs positions of the RB model. In each of these cases, the power-law exponents of geometrically-related SM and RB parameters are within three standard deviations of one another.

Based on Landau and renormalization-group theory considerations, ISODISPLACE determined that none of the DT5+, SM2 or L2+ order parameters of the $CsFeO_2$ distortion are capable of producing continuous transitions when acting alone, and certainly not when acting simultaneously. Though the transition appears to be approximately second order in nature, first-order distortions that evolve too quickly below

the transition do provide a simple explanation the unusually-small power-law exponents that we observe.

Conclusions

We have demonstrated the semiautomated parametric refinement of structural order parameters that arise at the cubic-orthorhombic structural phase transition of $CsFeO_2$. This parametric refinement against diffraction patterns collected over a wide range of temperatures yielded power-law exponents and coefficients describing the evolution of the atomic displacements and the ferroelastic lattice-strains that contribute to the distortion. Two different parameterizations of the distortion, the symmetry-adapted distortion mode description and the internal rigid-body (i.e., z-matrix) description, proved to be closely related due to the natural tendency of symmetry modes to produce polyhedral tilts like those observed in $CsFeO_2$. With both models, the automated parametric refinement greatly increased the speed of the refinement and post-refinement analysis. To characterize power-law trends in structural order parameters, it was crucial to collect diffraction patterns at a sufficient number points above and below the phase transition, which is routinely possible at modern synchrotron sources. In the case of the present work, the interpretation of the power-law exponents was difficult due to fact that this structural phase transition is weakly first order. Yet, the parametric Rietveld refinement of symmetry modes and internal rigid body parameters as a function of external variables proved to be a powerful tool for investigating structural phase transitions. The principle benefit lies in the flexibility and convenience of identifying, testing and comparing candidate order parameters. The development of third party software for further automation of this rather complicated process is under way.

In Collaboration with:
B.J. Campbell (Brigham Young University, USA)

[1] *Salje, E.K.H.* Phase transitions in ferroelastic and co-elastic crystals. Cambridge University press (1990).

[2] *Stinton, G.W and J.S.O. Evans.* Journal of Applied Crystallography **40**, 87–95 (2007).

[3] *Campbell, B.J., H.T. Stokes, D.E. Tanner and D.M. Hatch.* Journal of Applied Crystallography **39**, 607–614 (2006).

[4] *Campbell, B.J., J S.O. Evans, F. Perselli and H.T. Stokes.* IUCr Computing Commission Newsletter **8**, 81–95 (2007).

[5] *Nuss, J., N.Z. Ali and M. Jansen.* Acta Crystallographica B **63**, 719–725 (2007).

[6] TOPAS, V.4.1; Bruker AXS.

Predicting crystalline solids exploring energy landscapes on ab initio level

K. Doll, J.C. Schön and M. Jansen

One of the great challenges in preparative solid state chemistry is the transformation of the field from an inductive to a deductive science by predicting the stable compounds, and their polymorphic modifications, for a chemical system and subsequently achieving their synthesis. These possible structures correspond to the locally ergodic regions on the energy landscape of the chemical system, i.e., the hypersurface of the potential energy as function of the atom arrangements. At low temperatures, these regions can be associated with individual minima on the landscape, while at elevated temperatures they often encompass many (closely related) minima. Over the past two decades [1], we have developed a general methodology to predict solid